

Oxygen behavior in aluminum nitride

M. Kazan

Groupe d'Etude des Semiconducteurs, CNRS-UMR 5650, cc 074, Université Montpellier II, 34095, Montpellier, France

B. Rufflé

Groupe Physique des Verres and Spectroscopies Laboratoire Colloïdes, Verre et Nanomatériaux Université Montpellier II-CC 069, 34095 Montpellier, France

Ch. Zgheib and P. Masri

Groupe d'Etude des Semiconducteurs, CNRS-UMR 5650, cc 074, Université Montpellier II, 34095, Montpellier, France

(Received 26 July 2005; accepted 24 October 2005; published online 30 November 2005)

The infrared lattice-vibration spectra of three polycrystalline samples of wurtzite AlN differing in their oxygen contamination have been studied by measuring the room-temperature reflectivity at near-normal incidence in the 400-3000 cm^{-1} frequency range using unpolarized light. A type of highly-contaminated-material reflectivity spectrum has been observed. Two-mode behavior has been observed at low oxygen concentration, one-mode behavior tends to be dominant when the oxygen concentration increases and only one-mode behavior has been observed at high oxygen concentration. Otherwise, a careful analysis of the data using the Kramers-Kronig technique and classical dispersion theory gives, in addition to the transverse and longitudinal mode frequencies, two in-band resonance modes attributed to oxygen point defects in AlN. Changes in the frequencies of these modes with oxygen concentration are interpreted as a transition in the oxygen accommodation defect as the concentration of oxygen increases. A model for the behavior of oxygen in AlN is proposed. © 2005 American Institute of Physics. [DOI: [10.1063/1.2137461](https://doi.org/10.1063/1.2137461)]

INTRODUCTION

Aluminum nitride has recently attracted much attention due to its optoelectronic material properties, characterized by its wide band gap (6 eV), which enable applications emitting short wavelength [blue ultraviolet (UV)] light. The interest in AlN stems also from the properties of its alloys with GaN which may permit the fabrication of AlGaN based optical devices which are very active from the blue wavelengths well into the ultraviolet. Each of these potential applications requires, among other factors, an understanding of the nature of native defects in the material because the defect-induced electronic states in the band gap can significantly alter the optical performance. This fact becomes extremely important in laser devices, where parasitic components in the emission spectrum are highly undesirable.

Oxygen-related defect complexes are important intrinsic defects in AlN ceramics. However, the local atomic structure of the oxygen point defect in AlN is still a critical issue. Theoretical^{1,2} investigations have shown that oxygen acts as a deep center due to the wide band gap of AlN and found it to easily substitute for the nitrogen atom in several charge states. Experimentally,^{3,4} it has been shown that a change in the nature of the oxygen defect occurs above a critical value of oxygen concentration. The model that has been proposed postulates that, at concentration below 0.75 at. %, the oxygen substitutes for nitrogen in the lattice, with one aluminum vacancy occurring for every three substituted oxygen atoms. Above 0.75 at. % a new type of defect is stable, in which an

aluminum atom is octahedrally bound to an increasing number of oxygen atoms. No oxygen substitution for aluminum in the lattice has been reported.

While impurities can be seen in infrared spectra via their local vibrational mode, in order to describe the oxygen behavior in AlN, we report an interpretation of measurements of the reflectivity spectra of polycrystalline AlN in the infrared reststrahlen region. Throughout the oxygen contamination range (~ 1 at. %, ~ 2 at. %, > 5 at. %) of the three samples investigated, the reflectivity spectrum shows two reststrahlen bands: (i) a strong band which is shifted down in frequency monotonically as the oxygen contamination increases and (ii) a higher frequency weak band which appears only at low oxygen contamination (~ 1 at. %) which weakens when the oxygen contamination increases (~ 2 at. %) and vanishes completely at high oxygen contamination (> 5 at. %). The vanishing of the high frequency weak band is accompanied by the appearance of a weak structure near 890 cm^{-1} , which increases in magnitude with increasing oxygen contamination. It should be noted that a deformation at the lower edge of the main reststrahlen band occurs at low oxygen contamination (~ 1 at. %). All these changes in the reststrahlen band with oxygen concentration are interpreted as a transition in the oxygen defect accommodations as the concentration of oxygen increases.

We propose in this work a model based on changes occurring in the reststrahlen band response throughout the oxygen contamination range of the three samples investigated, in which we postulate that oxygen can exist in AlN in four

structures and the existence of each structure depends on oxygen concentration and nitrogen vacancies.

EXPERIMENT

The AlN crystals investigated here are grown by sublimation of an AlN charge placed in the hot zone of a tungsten crucible and subsequent condensation of vapor species in a cooler region. The details of the growth procedure are discussed elsewhere.⁵ Secondary ion mass spectroscopy (SIMS) measurements indicate that oxygen is the only significant impurity and the concentration of Al and N is similar in the three samples. High-quality surfaces for Fourier transform infrared (FT-IR) measurements were prepared by chemical polishing, which was performed in an identical way for all the AlN samples to remove the oxide films immediately prior to the measurements.

The reflectivity spectra were taken at room temperature in the 400–3000 cm^{-1} frequency range using a Bruker IFS 66V spectrometer which supplies an FT-IR microscope operating in reflectivity mode. A KBr beamsplitter and a DTGS detector with a resolution of less than 1 cm^{-1} were used. The light was unpolarized and at near-normal incidence. The reflectivity of the samples was compared with that of a gold-coated mirror with an assumed reflectance of 0.98. The samples investigated present large areas (1 $\text{cm} \times 1 \text{ cm}$) and smooth surfaces compared with the wavelengths used in our study, so that normalization of the spectra was not necessary.

RESULTS AND DISCUSSION

One can distinguish two types of behavior in crystals containing a high concentration of impurities such as AlN (which seems to present an extreme case in this respect, because of the possibility of several percent oxygen incorporation⁴): One-mode behavior occurs when the impurity local vibration mode lies within the reststrahlen band of the host crystal. In this case, the reflectivity spectra exhibit a single reststrahlen band. In contrast to this, two-mode behavior occurs when the impurity local vibration mode lies out of the reststrahlen band of the host crystal: here two reststrahlen bands must be observed. The behavior we report here represents a type of highly contaminated-crystal reststrahlen band response, which is a combination of the one- and two-mode systems discussed earlier.

In Fig. 1, we present the reflectivity spectra of the three AlN polycrystals samples investigated. The reflectivity spectrum of the purest sample shows a deformation in the lowest edge of the main reststrahlen band, a weak structure near 890 cm^{-1} and an additional high frequency weak band. With increasing oxygen concentration, the deformation at the lowest edge of the main reststrahlen band disappears, the weak structure near 890 cm^{-1} increases in magnitude and the high frequency weak band weakens until it vanishes completely, while the strong reststrahlen band shifts downwards.

The reflectivity spectra were analyzed using a Kramers-Kronig dispersion analysis. The Kramers-Kronig integral permits at each frequency the determination of the optical constants n and k or alternatively ϵ_1 and ϵ_2 , the real and the imaginary parts of the complex dielectric constant, from the

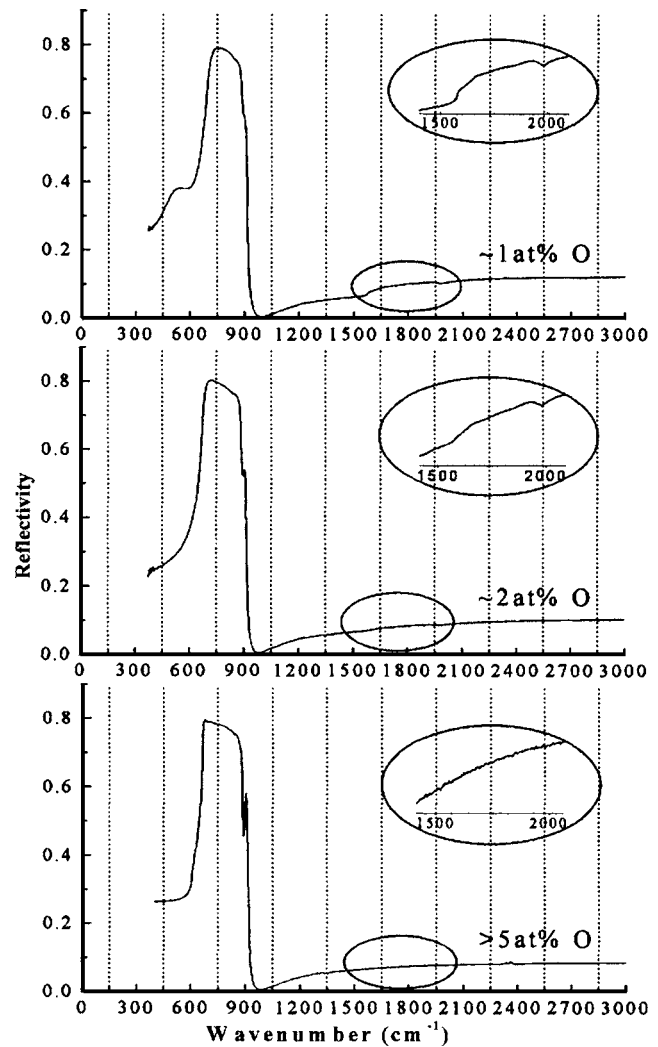


FIG. 1. Reflectivity spectra of the three AlN polycrystals investigated. The inset shows the behavior of an additional reststrahlen band throughout the oxygen contamination range of the three samples investigated.

knowledge of the reflectivity spectrum only. The frequencies of the maxima of ϵ_2 and $\text{Im}(-1/\epsilon)$ are taken to correspond, respectively, to the TO phonon and to the LO phonon frequencies. In order to understand the changes in the reflectivity spectra, a best fit to the three ϵ_2 and $\text{Im}(-1/\epsilon)$ plot was performed. The best fit, as judged by the least-squares analysis and by visual inspection, was obtained by a three-Lorentzian-fit to each ϵ_2 and $\text{Im}(-1/\epsilon)$ plot. The best fit to each ϵ_2 plot shows one strong peak and two additional weak peaks. In the following, the strong peak will be referred to as TO while the two additional weak peaks will be referred to as TO₁ and TO₂. Similar to the ϵ_2 plots, the best fit to each $\text{Im}(-1/\epsilon)$ plot shows one strong peak and two additional weak peaks. The strong peak will be referred to as LO while the two additional weak peaks will be referred to as LO₁ and LO₂. The TO and LO frequencies are supposed to be, respectively, the transverse and the longitudinal optic modes of the host crystal, while the other frequencies are treated in terms of in-band resonance modes. The best fits to the ϵ_2 and $\text{Im}(-1/\epsilon)$ plot of the purest sample was obtained with three Lorentzians ignoring the deformation at the lowest edge of the main reststrahlen

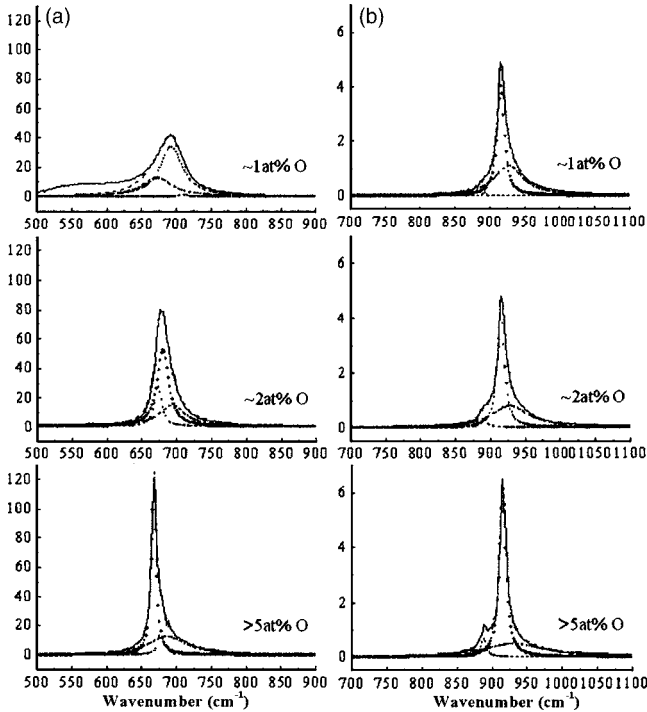


FIG. 2. Optical parameters calculated from the reflectivity data. (a) Solid line: plot of ϵ_2 . Dashed line: best fit to the calculated ϵ_2 in terms of three Lorentzian shown in dotted lines. (b) Solid line: plot of $\text{Im}(-1/\epsilon)$. Dashed line: best fit to the calculated $\text{Im}(-1/\epsilon)$ in terms of three Lorentzians shown in dotted lines. The Lorentzian best fit to ϵ_2 and $\text{Im}(-1/\epsilon)$ shows the behavior of the optic mode and two in-band resonance mode frequencies throughout the range of oxygen concentration in AlN.

band, for the following set of values: $\text{TO}=693.6\text{ cm}^{-1}$, $\text{TO}_1=673.5\text{ cm}^{-1}$, $\text{TO}_2=710.1\text{ cm}^{-1}$, $\text{LO}=916.3\text{ cm}^{-1}$, $\text{LO}_1=927.4\text{ cm}^{-1}$, $\text{LO}_2=892.3\text{ cm}^{-1}$. With increasing oxygen concentration, the LO and TO shift downwards. At high oxygen concentration, when the higher frequency weak band vanishes completely, only one-mode behavior is observed and, the TO mode acquires the reported value³⁻⁶ of the AlN transverse optical mode. With increasing oxygen concentration, the set of frequencies (TO_1 and LO_1) shifts from values close to the reported⁷ TO and LO frequencies of Al_2O_3 to higher frequencies, and the second set of frequencies (TO_2 and LO_2) shifts downwards. This shift of the two set of frequencies is accompanied by a decrease of the areas under the TO_1 and the LO_1 peaks, an increase of those under the TO_2 and LO_2 peaks and a vanishing of the high-frequency weak band. The behavior throughout the range of oxygen concentration of the phonon frequencies and the in-band resonance

modes derived from the ϵ_1 and ϵ_2 curves resulting from the Kramers-Kronig analysis is shown in Fig. 2(a) and 2(b) and tabulated in Table I.

The changes in the reststrahlen band as well as the occurrence of one- or two-mode behavior are well understood on the basis of local-mode theory. The criteria for two-band behavior are that, in the heavier ion compound, the local mode due to the substituted ion must fall above the optical branch of the host crystal spectrum and that, similarly, in the lighter ion compound, the substituted impurity ion must give rise either to a localized gap mode between the acoustical and optical branches of the parent crystal, or to an in-band resonance mode. Moreover, in a two-mode system the LO frequency of the host crystal increases and its TO frequency decreases as the concentration of the impurity substituting the heavier ion compound decreases. In contrast to this, in a typical one-mode system both frequencies of the host crystal shift in the same sense as the concentration of impurity substituting the lighter ion compound decreases.

One criterion for in-gap localized mode and consequently two-mode behavior is that the phonon dispersion of the host crystal be such that a gap does exist between its acoustical and optical branches. In other words, the density of phonon states must be very low between the acoustical and optical branches. AlN in the wurtzite structure does not have such a gap,⁸ and it therefore follows that any impurity with an atomic mass larger than that of nitrogen that substitutes for nitrogen cannot exhibit the conventional two-mode behavior. Therefore, strict one-mode behavior is possible when an impurity with a larger atomic mass than that of nitrogen substitutes for nitrogen. We attribute the deformation at the lower edge of the main reststrahlen band observed in the reflectivity spectra of the purest sample to an in-band resonance mode within the 252 (E_2 frequency)-400 cm^{-1} range frequency caused by nitrogen vacancies substituted by oxygen atoms. Observation of the reflectivity spectra in this frequency range was not possible because it was out of the limit of our detector. It should be noted that this shape of the reststrahlen band has been observed in the behavior of $\text{Ga}_{1-x}\text{In}_x\text{As}$ (Ref. 9) at low values of x when the In atom (which has a larger atomic mass than that of Ga atom) constitutes an impurity substituting for the Ga atom (which is the lighter atom). From what was discussed earlier, the two-mode behavior and consequently the high-frequency weak reststrahlen band which appears at the same time as the one-mode behavior in the reflectivity spectrum of the purest sample is attributed to an aluminum vacancy substituted by

TABLE I. Summary of the best fit to the Kramers-Kronig calculations throughout the oxygen concentration range (~ 1 at. %, ~ 2 at. %, and > 5 at. %) for all investigated samples. Freq. indicates the position of each in-band resonance mode, while Area indicates the area under each Lorentzian attributed to an in-band resonance mode.

Oxyg. % (at. %)	TO (cm^{-1})	LO (cm^{-1})	TO ₁		LO ₁		TO ₂		LO ₂	
			Freq. (cm^{-1})	Area (a.u.)	Freq. (cm^{-1})	Area (a.u.)	Freq. (cm^{-1})	Area (a.u.)	Freq. (cm^{-1})	Area (a.u.)
~ 1 at. %	693.6	916.3	673.5	1031.0	927.4	84.6	710.1	22.7	892.3	0.6
~ 2 at. %	682.0	916.2	674.4	556.7	928.7	80.9	694.1	1094.9	891.7	4.4
> 5 at. %	668.8	915.9	679.4	248.9	931.8	75.9	688.3	1246.8	889.1	9.2

oxygen (which has a smaller atomic mass). The set of frequencies (TO_1 and LO_1) is attributed to layers of stressed Al_2O_3 in the host crystal. The set of frequencies (TO_2 and LO_2) is attributed to layers of Al_2O_x where $x > 3$. The change of the reststrahlen band and the vanishing of the high frequency weak band as well as the alternation of the magnitude of the in-band resonance modes are attributed to a transition in the oxygen accommodation defect as the concentration of oxygen changes. Also, from what is discussed earlier, the shift of the TO from 693.6 cm^{-1} downwards to the reported value with increasing oxygen concentration is well understood on the basis of the vanishing of the contribution of the two-mode behavior and the occurrence of only one-mode behavior at high oxygen concentration.

All these observations strongly suggest that when oxygen enters the AlN structure, three oxygen atoms substitute for three nitrogen atoms and form layers of Al_2O_3 with two dangling bonds on the Al atoms. When all the dangling bonds of the Al atoms are compensated, oxygen substitutes for the aluminum atoms and for nitrogen atoms but this time without forming the Al_2O_3 structure but rather respectively Al-O-Al and N-O-N configurations. At very high oxygen concentration, when all the nitrogen and aluminum vacancies are compensated, the N-O-N, Al-O-Al, and the Al_2O_3 bonds break successively, and an increased number of oxygen atoms group together around the two dangling bonds of the Al atoms and forms layers of Al_2O_x , where x is an integer > 3 .

CONCLUSION

In conclusion, we have shown that oxygen-contaminated AlN samples present a type of contaminated-material behavior, in which a combination of the one- and two-mode be-

havior can be observed in its reflectivity spectra. We have related the changes of the behavior of the reflectivity spectra to several structures formed by oxygen in wurtzite AlN. Each structure has been found to depend on oxygen concentration and nitrogen vacancies in the sample investigated. FT-IR spectroscopy can be a nondestructive technique for detecting point defects and oxygen concentrations in AlN via the behavior of the reflectivity spectra of the sample. The reflectivity measurements involving the temperature factor or coupled to other experiments such as electron paramagnetic resonance (EPR) can lead to a better understanding of the defect species present in AlN.

ACKNOWLEDGMENTS

The authors would like to thank Erlangen University (UEN-IMS6 group) for providing samples. The authors also gratefully acknowledge "Le Conseil Régional Languedoc-Rousillon" for supporting this study. The authors would like to thank L. McNeil for helpful discussions and for critical reading of this manuscript.

¹T. Mattila and R. M. Nieminen, Phys. Rev. B **54**, 16676 (1996).

²Q. Hu, T. Noda, H. Tanigawa, T. Yoneoka, and S. Tanaka, Nucl. Instrum. Methods Phys. Res. B **191**, 536 (2002).

³L. E. McNeil, M. Grimsditch, and R. H. French, J. Am. Ceram. Soc. **76**, 1132 (1993).

⁴R. A. Youngmand and J. H. Harris, J. Am. Ceram. Soc. **73**, 3238 (1990).

⁵B. M. Epelbaum, C. Seitz, A. Magerl, M. Bickermann, and A. Winnacker, J. Cryst. Growth **265**, 577 (2004).

⁶A. T. Collins, E. C. Lightowlers, and P. J. Dean, Phys. Rev. **158**, 833 (1967).

⁷M. Schubert, J. E. Tiwald, and C. M. Herzinger, Phys. Rev. B **61**, 8187 (2000).

⁸H. M. Tütüçü and G. P. Srivastava, Phys. Rev. B **62**, 5028 (2000).

⁹M. H. Brodsky and G. Lucovsky, Phys. Rev. Lett. **21**, 990 (1968).